

Supplementary Data

Pharmacokinetic/pharmacodynamic modeling to predict antiplatelet effect of ticagrelor-loaded self-microemulsifying drug delivery system in rats

Young-Guk Na,^{†,‡} Jin-Ju Byeon,^{†,‡} Min-Ki Kim,[†] Min-Gu Han,[†] Cheong-Weon Cho,[†] Jong-Suep Baek,^{,§} Hong-Ki Lee,^{*,†} Young G Shin,^{*,†}*

[†]College of Pharmacy, Chungnam National University, 99 Daehak-ro, Yuseong-gu, Daejeon 34134, Republic of Korea

[§]Department of Herbal Medicine Resource, Kangwon National University, 346 Hwangjo-gil, Dogye-eup, Samcheok-si, Gangwon-do 25949, Republic of Korea

[‡]These authors contributed equally.

*Correspondence: Jong-Suep Baek, College of Pharmacy, Department of Herbal Medicine Resource, Kangwon National University, 346 Hwangjo-gil, Dogye-eup, Samcheok-si, Gangwon-do 25949, Republic of Korea

E-mail: jsbaek@kangwon.ac.kr. Tel: +82-33-540-3320. Fax: +82-33-540-3329

*Co-correspondence: Hong-Ki Lee, College of Pharmacy, Chungnam National University, 99 Daehak-ro, Yuseong-gu, Daejeon 34134, Republic of Korea

E-mail: hk_lee@cnu.ac.kr. Tel: +82-42-821-7301. Fax: +82-42-823-6566

*Co-correspondence: Young G Shin, College of Pharmacy, Chungnam National University, 99 Daehak-ro, Yuseong-gu, Daejeon 34134, Republic of Korea

E-mail: yshin@cnu.ac.kr. Tel: +82-42-821-5931. Fax: +82-42-823-6566

1. Supplementary methods

1.1. LC-MS/MS analysis of TCG

The concentrations of TCG were determined using a liquid chromatography tandem-mass spectrometry (LC-MS/MS) system consisting of Agilent 1290 series and Agilent 6495 Triple Quad LC/MS (Agilent Technologies, Santa Clara, CA, USA). A YMC-Triart C18 column (50 × 2.0 mm, 1.9 μm; YMC Inc., Wilmington, NC, USA) was used as a chromatographic column. The mobile phase consisted of solvent A (0.1% formic acid in distilled water) and solvent B (0.1% formic acid in acetonitrile), with a gradient elution (0–0.5 min, 10% solvent B; 0.5–1.0 min, 10% to 95% solvent B; 1.0–1.5 min, 95% solvent B; 1.5–1.6 min, 95 to 10% solvent B; 1.6–3.0 min, 10% solvent B). The flow rate was 0.4 mL/min and the injection volume was 10 μL. The temperature of the column and autosampler were set as 30 °C and 4 °C, respectively. The positive ion mode using Agilent jet stream electrospray ionization (AJS-ESI) was applied to record the scan mass spectra. The ion transitions of TCG and verapamil (ISTD) were set as 523.1→153.0 m/z and 455.3→165.1 m/z, respectively, and detected with a multiple reaction monitoring (MRM) mode. The collision energies for TCG and ISTD were 40 V and 30 V, respectively. The cell accelerator voltage was 5 V and the dwell time was set as 200 ms. The source parameters were set as follows: Gas temperature 200°C, gas flow 14 L/min, nebulizer 20 psi, sheath gas heater 250°C, sheath gas flow 11 L/min, capillary 3000 V, and nozzle voltage 1500 V.

In this analysis, the most abundant ion transition of TCG (523.1→153.0 m/z) was selected to determine the lowest limit of quantification (LLOQ), and the LLOQ of TCG was 3 ng/mL. The range of calibration curve of TCG was set to 3–6600 ng/mL. The curve was written with a weighted linear regression ($1/x^2$) and showed excellent linearity with $R^2 > 0.999$. The method has shown accurate and reproducible results within acceptable tolerances (less than 20% coefficient of variation (CV) at LLOQ and less than 15% CV at all other concentrations). The acquired LC-MS/MS data were processed with Agilent analysis software (Agilent MassHunter Quantitative Software Version B.07.00).

2. Supplementary results

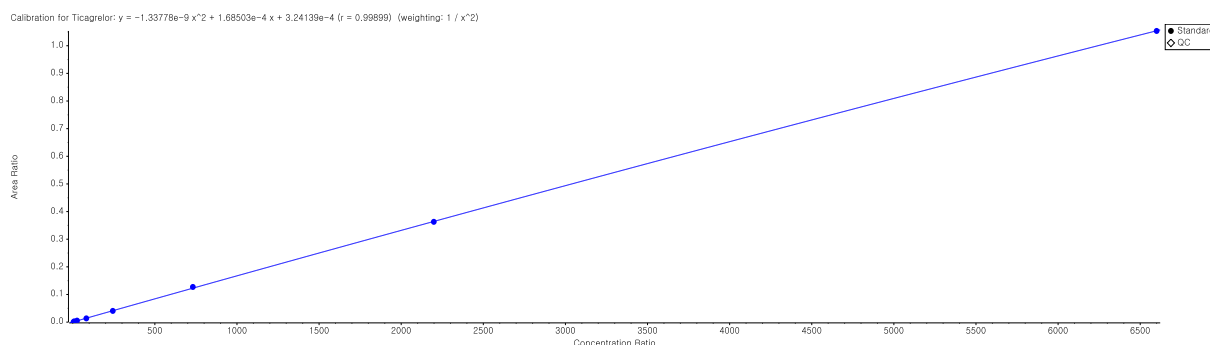


Figure S1. Calibration curve of ticagrelor (concentration range 3–6600 ng/mL).

Table S1. Ticagrelor concentration in standard samples measured by LC-MS/MS analysis.

Actual concentration (ng/mL)	Area	Calculated concentration (ng/mL)	Accuracy (%)
3.02	39.65	3.09	102.19
9.05	87.55	8.35	92..23
27.16	265.3	27.76	102.19
81.48	805.3	85.72	105.20
244.44	2114	34.90	96.10
733.33	6044	752.45	102.61
2200	18140	2189.89	99.54
6600	55180	6595.73	99.94

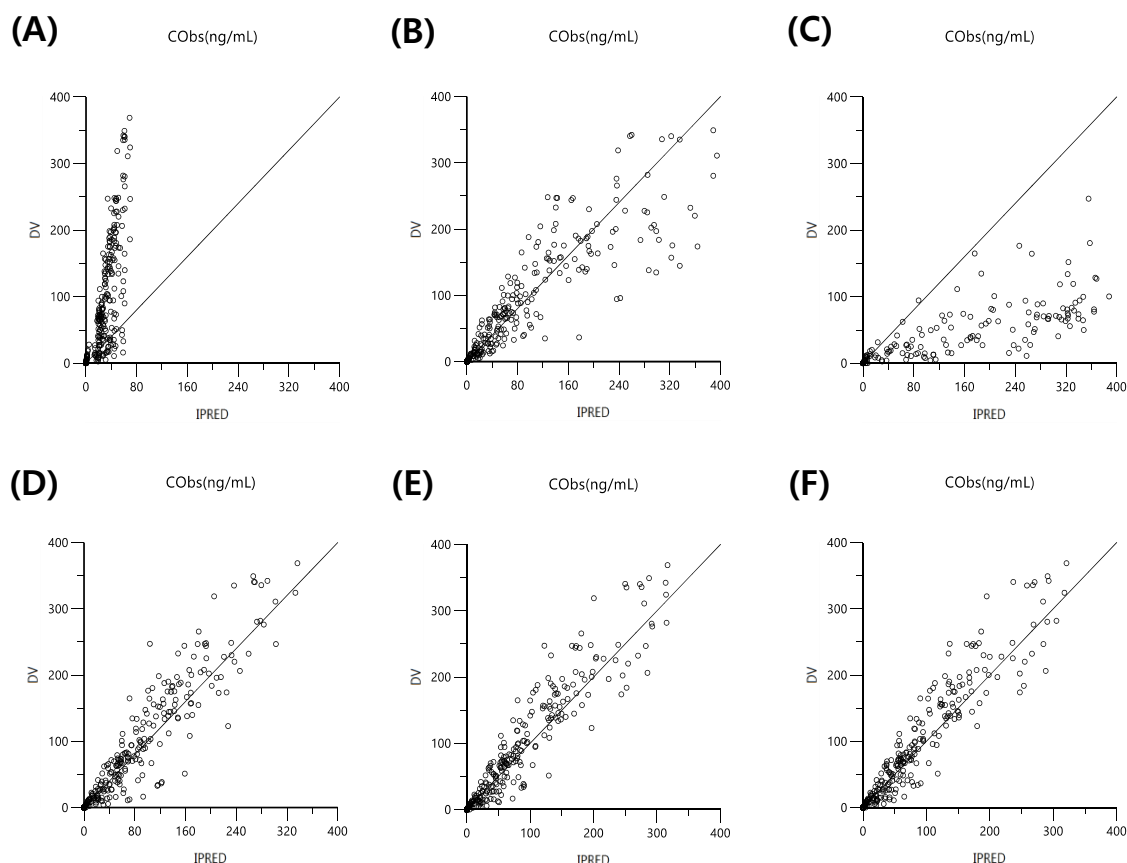


Figure S2. Goodness-of-fit plots of (A) one-compartment model with saturated absorption, (B) one-compartment model with multi-absorption compartments, (C) one-compartment model with saturated elimination, (D) one-compartment model with linear-decreased F value, (E) two-compartment model, and (F) one-compartment model. The dotted marks indicate the observed data. The solid line represents the line of unity.

Table S2. Objective function values (OFV) from different PK models.

PK models	OFV (-2LL)
One-compartment model with saturated absorption	2512.32
One-compartment model with multi-absorption compartments	2417.01
One-compartment model with saturated elimination	2900.25
One-compartment model with linear-decreased F value	2402.75
Two-compartment model	2277.95
One-compartment model	2395.59

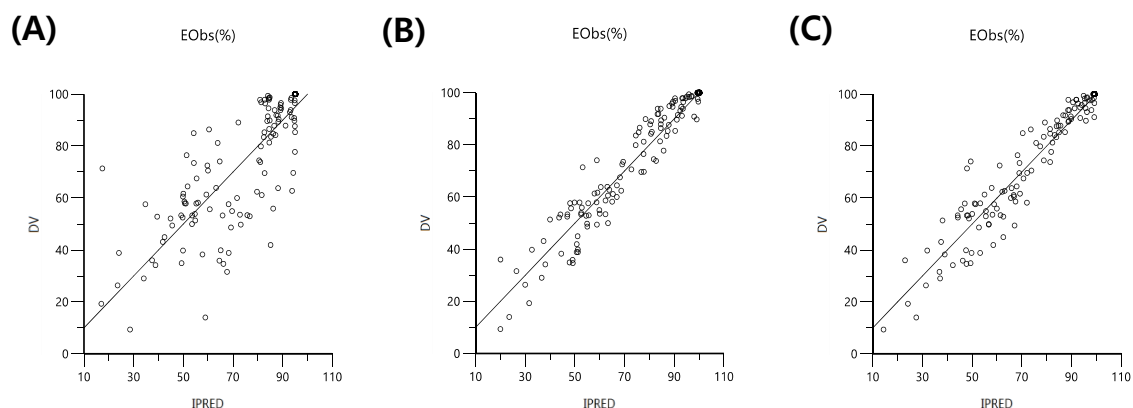


Figure S3. Goodness-of-fit plots of (A) direct response E_{\max} model, (B) effect compartment model, and (C) indirect response E_{\max} model. The dotted marks indicate the observed data. The solid line represents the line of unity.

Table S3. Objective function values (OFV) from different PK/PD models.

PK/PD models	OFV (-2LL)
Direct response E_{\max} model	1327.67
Effect compartment model	1174.58
Indirect response E_{\max} model	1182.10

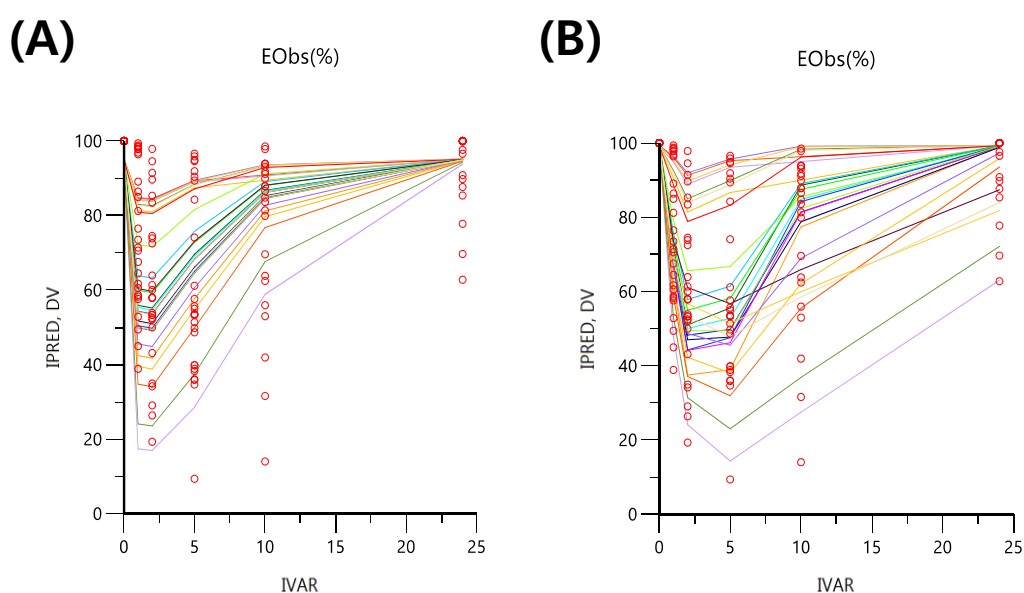


Figure S4. Observed data and model-simulated data by (A) effect compartment model and (B) indirect response E_{\max} model. The dotted marks and solid lines represent the observed data and the simulated profiles, respectively.

- **Results:** The effect compartment model showed lowest OFV, but the model could not reflect the I_{\max} and the observed effect at 10 h. So, we selected the two-compartment model as a final population PK model.